Earth Planets Space, **59**, 853–862, 2007

A new type of a three-component spinner magnetometer to measure the remanence of rocks at elevated temperature

Michael Wack and Jürgen Matzka*

Department of Earth and Environmental Sciences, Ludwig-Maximilians-Universität München, Theresienstr. 41, 80333 Munich, Germany

(Received September 30, 2006; Revised February 23, 2007; Accepted February 23, 2007; Online published July 20, 2007)

A new instrument to continuously determine the remanent magnetisation of standard paleomagnetic (inch-sized) rock samples during heating and cooling (continuous thermal demagnetisation) was developed. The design as an off-axis spinner magnetometer (i.e. the samples rotate on a circular path in a radial distance to the spinning axis) allows the simultaneous measurement of several samples and offers a way to determine the full vector of magnetisation. Six fluxgate sensors are used to record three gradients of the magnetic fields caused by the samples and the vector of remanence is determined by regression analysis of the gradient signals. The sensitivity of the instrument is $2 \cdot 10^{-7}$ Am^2. Hot air is circulating through copper pipes which heat the samples by thermal radiation to avoid magnetic fields which would arise from direct electrical heating. Currently, the measurements are restricted to a maximum of 350°C. The instrument was tested with oceanic basalt samples that were given an artificial remanence. Some continuous thermal demagnetisation experiments of this artificial remanence and of the natural remanent magnetisations are shown for oceanic basalts.

Key words: Spinner magnetometer, fluxgate, continuous thermal demagnetisation, natural remanent magnetisation, partial self-reversal, oceanic basalt, DSDP/ODP, Hotspin.

1. Introduction

Thermal demagnetisation of rock samples can be done in two ways (Collinson, 1983). The difference is the temperature at which the magnetisation of the specimens is measured. The stepwise method (e.g. Irving *et al*., 1961; Stephenson, 1967) is based on the determination of the magnetisation at room temperature after heating the sample to a certain temperature and cooling in zero field. This procedure must be repeated for each temperature step. The advantage is that many samples can be heated together under similar conditions. The other approach is to determine the magnetisation continuously (e.g. Stacey, 1959; Creer, 1967; Chamelaun and Porath, 1968) during heating and cooling of the specimen. Therefore, only one heating and cooling process is necessary and effects like (partial) self-reversal (Krása *et al*., 2005) or multidomain effects (McClelland and Sugiura, 1987; Shcherbakov *et al*., 1993) of the magnetic remanence or changes in the magnetic behaviour due to thermal alteration can be investigated. Results of the two methods can show systematical differences both in the intensity and in the directions, which are important in paleomagnetism. When measuring magnetic remanences at elevated temperature, a modulation of its intensity by the temperature dependency of the spontaneous magnetisation $M_S(T)$ has to be taken into account. This might lead to erroneous determinations of paleomagnetic directions as shown by Schmidt and Clark (1985). Generally, the remanences measured close to the Curie temperature are weaker than at room temperature, necessitating a more sensitive magnetometer.

Currently, several rock and paleomagnetic laboratories are operating rock magnetometers to measure magnetic remanence at elevated temperature. For example, the Geophysical Observatory Borok has a self-built two-component induction coil spinner magnetometer with a sensitivity of $3 \cdot 10^{-9}$ Am^2 and measurements up to 600°C are shown in Shcherbakova *et al*. (2000). A second instrument there is a three-component thermal magnetometer with a sensitivity of $1 \cdot 10^{-8}$ Am^2. Both instruments operate with 1 cm^3 sized samples (pers. comm. V. Shcherbakov). The Institut de Physique du Globe de Paris has a self-built three-component vibrating sample magnetometer with a sensitivity of $1 \cdot 10^{-8}$ Am^2 and a maximum temperature of 650°C. It has an electric heating with maximum heating rates of 60°C per minute and has several special features that allow paleointensity determinations (Le Goff and Gallet, 2004; Gallet and Le Goff, 2006). A vibrating sample magnetometer for one component is located at the Université Montpellier 2 and is used for rock magnetic and paleointensities studies (e.g. Plenier *et al*., 2003; Dräger *et al*., 2006). The instrument with a sensitivity of $2 \cdot 10^{-9}$ Am^2 operates between −192°C and 700°C (pers. comm. P. Camps). A self-built astatic magnetometer to measure one component of remanence at temperatures of up to 600°C is located at the Ecole Normale Supérior in Paris. This instrument also allows experiments under controlled pressure (Cairanne *et al*., 2003).

The above mentioned instruments demonstrate that for

*Now at: Danish Meteorological Institute, Lyngbyvej 100, DK 2100 Copenhagen, Denmark.

the measurement of one or two components of magnetisation both vibrating sample and spinner magnetometers are used. For the automatic measurement of the full vector of magnetisation, usually vibrating sample magnetometers are used, since conventional spinner magnetometers are restricted to the measurement of two components only. A notable exception are the novel types of spinner magnetometers that were developed by Masaru Kono. Kono *et al*. (1981) have described a new type of spinner magnetometer, able to measure the full vector of magnetisation by rotating the sample simultaneously with different speed around two perpendicular axes. Kono *et al*. (1991) further developed this method by combining rotation and translation of the sample with a simple mechanical set up for the sample holder. This simple sample holder could be automatically moved from a furnace to a ring core fluxgate sensor (Kono *et al*., 1984) for automatic stepwise thermal demagnetisation.

2. Instrumentation

Our new magnetometer 'Hotspin 2' is an advanced version of the already existing 'Hotspin' instrument (Matzka, 2001) which was previously used to study oceanic basalt magnetomineralology (Matzka *et al*., 2003; Krása and Matzka, 2007; Matzka and Krása, in press). Hotspin, like all conventional spinner magnetometers, is limited to the measurement of only two of three components of a sample's magnetisation. The sample is rotated around one of its principle axes and the sinusoidal variation of the magnetic field of the remanence component perpendicular to the rotational axis is measured and then the remanence's intensity and phase is determined by fourier transform from the sinusoidal signal. The signal can be stacked over several rotations and the sensor offset is irrelevant to this procedure. Hotspin 2 provides the same advantages, namely stacking of the signal and independence of individual sensor offsets. However, the new instrument is an off-axis spinner magnetometer, which means that the samples are mounted at a radial distance to the rotation axis (in this sense, it is similar to a vibrating sample magnetometer, but with a circular instead of a linear path of the sample). On their circular path, the samples are passing six fluxgate senors and three magnetic field gradients as well as the samples' positions are continuously recorded. The best fitting magnetic dipole to this signal is determined by linear regression. This allows the determination of all three components of magnetisation, which is essential to obtain the full paleomagnetic information, without the need for a mechanism to turn the samples around an axis perpendicular to the rotation axis as described for a high temperature spinner magnetometer of the conventional type by Heiniger and Heller (1976). Compared to existing magnetometers for continuous thermal demagnetisation, the new Hotspin 2 magnetometer has certain design characteristics that are specific to its use in studying the processes that affect magnetisation of oceanic basalts during thermal treatment. It must be able to measure the full vector of remanence, but the angular accuracy is not as critical as in paleomagnetic studies for geomagnetic or paleogeographical reconstructions. Nevertheless, an advantage to most other instruments, which use small rock samples difficult to orient, is the use of standard inch paleomagnetic samples. Hotspin 2 can be less sensitive than other instruments, since the samples to be studied are strongly magnetic basalts. An advantageous design characteristic of Hotspin 2 is also that simultaneously several samples and the temperature sensor are moved within an identical thermal environment, whereas usually other instrument always have the sample located at one point and the temperature sensor at another point. Finally, most instruments are designed to screen DC magnetic fields at the sample location, but still use an AC heating wire. Hotspin 2 is designed with a hot air heating to minimise AC magnetic fields that possibly could affect the samples magnetisation, e.g. close to the Curie point where magnetic stability is low. A clear disadvantage of the Hotspin 2 design is that relatively little experience exists on the use of hot air heating in paleomagnetism and reaching sufficiently high temperatures with this technology proofs to be the major design drawback. In the following, we describe Hotspin 2, a more detailed description of the instrument can also be found in Wack (2006).

2.1 Mechanical setup

All parts of the instrument which are close ($<$ 1 m) to the sensors or the samples are built of nonmagnetic materials like aluminium, copper, ceramics or glass. The ambient field is compensated by three orthogonal Helmholtz coils with a size of two meters surrounding the instrument. The specimens (standard inch cores) are located on holders made of quartz glass which are fixed on a rotating disc at a distance of 15 cm to its rotation axis in the disc's centre (Fig. 1(a)). The rotating disc is supported from above by a static central axis. The disc is driven via tooth belts and a rotating tube around the central axis by a dc-motor, mounted in a distance of 1.1 m to the sensors on a boom to minimise magnetic influence. For our measurements we use a rotating speed close to 7 rpm. The mountings for the specimen holders are arranged in such a way on the disc that a thermocouple and one, two, three or five samples can be installed at equal distances to each other. This guarantees the best separation of the magnetic signals. Whereas the samples are fixed to the rotating platform, the thermocouple is allowed to rotate on its position to exactly counteract the disc's rotation. As a consequence, the tip of the thermocouple is moving on the same circular path as the samples, but its orientation remains constant, preventing its cable from winding up. The top of the holders with the specimens and the tip of the thermocouple reside inside a stationary, toroidal-like oven (cross section in Fig. 1(b)), which is heated by hot air that is guided through copper pipes in the oven's side walls. The air is heated by a heat gun. The circulation of the hot air through the pipes is supported by a fan at the end. To avoid damage of the fan, a cooling unit was implemented to cool the air back to room temperature. The air system is closed inside the oven, so the actual sample heating is done through thermal radiation.

Figure 1(a) shows the central part of the instrument without the dc-motor, tooth belts, the heat gun and the fan. A cross section of the oven is shown in Fig. 1(b). The design of the instrument makes it possible to apply a defined magnetic field parallel to the rotation axis for additional experiments, e.g. the acquisition of thermoremanent magneti-

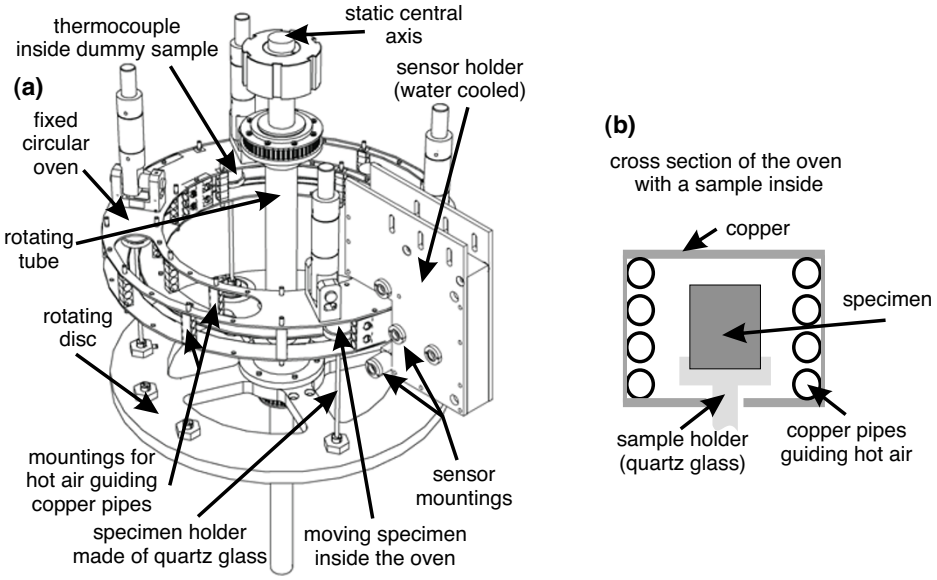

Fig. 1. Mechanical setup of Hotspin 2. For a more concise visualisation only the central part of Hotspin 2 without the walls of the oven or peripheral equipment is shown in (a). A cross section through the toroidal-like oven is presented in (b). Heating is done by hot air flowing through the copper pipes on the left and the right side.

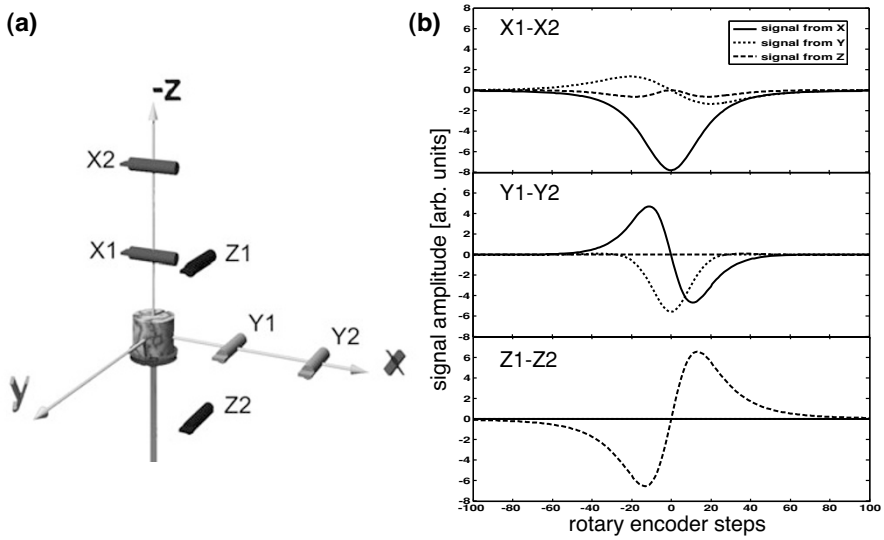

Fig. 2. Sensor geometry of Hotspin 2 (a) and calculated differential signals (b), see text.

sation during paleointensity studies.

2.2 Sensors and electronics

The six fluxgate sensors (MAG-03 from Bartington Instruments Ltd.) are incorporated in a sensor holder made of aluminium with internal water-cooling to protect the sensors. The sensors were chosen because of their high field resolution and small size (only 20 mm long). To reduce the influence on the measurement signal by temporal changes in the ambient fields, which can be substantial at our current location in the centre of Munich, differential signals of three pairs of sensors are used. This is taking advantage of the fact that the spatial gradient of magnetic noise from a remote source can be treated to be homogenous compared to the sample's magnetic field.

Prior to building the sensor holder, the expected differential fluxgate signals were calculated for various sensor geometries, from which an easy-to-manufacture sensor geometry was chosen that provides an approximately equally high sensitivity and a reasonably good seperation of all magnetisation components. The geometrical arrangement of the six fluxgate sensors (X1, X2, Y1, etc.) inside the sensor holder is shown with the instrument's coordinate system x, y, z in Fig. 2(a), where the y direction is tangential to the movement of the specimen. The sensors X1 and X2, for example, are simply located above the sample's path, in the second Gaussian position to the sample's magnetisation component X. Sensor X2 is further separated from the sample and will probe a smaller field than sensor X1. Sensors Y1 and Y2 are located in analogue positions. For Z1 and Z2, differential fluxgate signals for various sensor positions and orientations were calculated and compared with the differential fluxgate signals of the other sensors, with

the aim to achieve a similarly good sensitivity and separation of components. In this course, a position for Z1 and Z2 was found (Fig. 2(a)), that is even better in terms of differential signal amplitude and separation of the magnetisation's Z component than the sensors for the other components (see below). This configuration was finally chosen. For data analysis, differential signals of corresponding sensors are used (e.g. X1–X2). Each of the three differential signals is the sum of three elements caused by the different components X, Y, Z of the specimen's magnetisation vector. This is shown in Fig. 2(b). So X1–X2 is mainly influenced by the X-component of the magnetisation, Y1–Y2 by the X and the Y component and Z1–Z2 exclusively by the Z-component. The differential fluxgate signal of Z1 and Z2 adds constructively the signal of the sample's Z component magnetisation, resulting in the highest signal amplitude for this component with the X and Y component completely canceled. For a sample magnetised equally in all components X, Y and Z, the expected differential signals at each pair of sensors can be deduced from Fig. 2(b) by adding the respective full, dashed and dotted line.

The distance between the closest fluxgate sensor and the sample's center is 3.5 times the sample's radius (for standard inch paleomagnetic core). For this distance, and using the formulas in Collinson (1983, page 217) the magnetic field of a standard inch paleomagnetic core is deviating from a dipole by between 2 and 4%, translating into an angular difference of less then 2.5°. But note that the formulas are valid for certain geometries only (Collinson, 1983).

The variations of the differential signals are in the order of a few millivolts for samples with a typical magnetisation of a few A/m. These signals are strengthened by an instrumentation amplifier and filtered through a fifth order low pass IC (LTC1062 from Linear Technology, set to a cut-off frequency of 10 Hz). A sensitivity of $2 \cdot 10^{-7}$ Am^2 or 20 mA/m for inch-sized standard cylinders is achieved which basically represents the limits of the fluxgate sensors.

Position tracking of the specimen is done with a rotary encoder. A microcontroller board with a built-in 24 bit ADC was programmed to process the signals from the encoder and the differential sensor signals. A standard PC is connected by RS232 and records the datasets consisting of the sample position and the sensor signals.

The temperature is measured inside a dummy sample made of pyrophyllite with an integrated thermocouple of type R (Pt13Rh-Pt) which takes the same circular path inside the oven like the other specimens to achieve a similar temperature behaviour (see Section 2.1). The heat gun is controlled by a Eurotherm controller connected to the PC.

2.3 Software

We use a standard PC with a custom-made, LabView (National Instruments) based software to control the instrument and to process the data. Consecutive temperature steps can be programmed in advance and are executed without further user interference. Still, temperature steps can be modified and added during the experiment. For each rotation of the disc, 1500 sampled values (500 rotary encoder steps × 3 differential signals), a time stamp and the current specimen temperature are stored for subsequent evaluations in a binary format.

This binary data can be analyzed with another part of our software, allowing to stack the datasets of a defined number of rotations and allowing to choose the length of the datasets (i.e. angular interval which is used for the analysis of an individual sample) for each sample. Further, all parameters of the regression analysis (see Section 3) can be adjusted. The results include three components of magnetisation, inclination, declination, intensity and several error parameters for each temperature value. In case of stacking over a temperature range, the average temperature is used.

3. Regression Analysis

To obtain the magnetic moment of the samples, the recorded differential data of the sensors must be interpreted appropriately. All calculations are based on formula (1) describing the field of a magnetic dipole (e.g. Fließbach, 2000) and assume a point sized magnetic field sensor. The vector $\vec{m}$ is the magnetic moment of the specimen, $\vec{r}$ is the vector from the sensor $\vec{p}$ to the specimen and $\vec{B}$ is the resulting field at the sensor position. R corresponds to the radius of the samples' path. ϕ describes the angular offset of the considered specimen to the sensor plane.

$$\vec{B}(\vec{r}) = \frac{\mu_0}{4\pi} \frac{3\vec{r}\,(\vec{r}\cdot\vec{m}) - \vec{m}r^2}{r^5} \quad \text{with}$$
$$\vec{r} = \begin{pmatrix} r_x \\ r_y \\ r_z \end{pmatrix} = \begin{pmatrix} p_x - R\cdot\cos\phi \\ p_y - R\cdot\sin\phi \\ p_z \end{pmatrix} \tag{1}$$

Equation (1) can be written as a linear equation (2) describing the magnetic field at one position $\vec{p}$.

$$\vec{B}\,(\phi) = \check{I}\,(\phi)\cdot\vec{m} \tag{2}$$

$$\check{I}(\phi) = \frac{\mu_0}{4\pi}\frac{1}{r^5} \cdot \begin{pmatrix} 2r_x^2 - r_y^2 - r_z^2 & 3r_xr_y & 3r_xr_z \\ 3r_yr_x & 2r_y^2 - r_x^2 - r_z^2 & 3r_yr_z \\ 3r_zr_x & 3r_zr_y & 2r_z^2 - r_x^2 - r_y^2 \end{pmatrix} \cdot \begin{pmatrix} \cos\phi & \sin\phi & 0 \\ \sin\phi & \cos\phi & 0 \\ 0 & 0 & 1 \end{pmatrix} \tag{3}$$

To account for the differential signals of the sensors at different positions and orientations the matrix S (Eq. (4)) is used for the regression analysis. Herein $\check{I}_{ij}^{\,X1}$ means the element $\check{I}_{ij}$ calculated for the coordinates of sensor X1.

$$S(\phi) = \begin{pmatrix} \check{I}_{11}^{\,X1} - \check{I}_{11}^{\,X2} & \check{I}_{12}^{\,X1} - \check{I}_{12}^{\,X2} & \check{I}_{13}^{\,X1} - \check{I}_{13}^{\,X2} \\ \check{I}_{21}^{\,Y1} - \check{I}_{21}^{\,Y2} & \check{I}_{22}^{\,Y1} - \check{I}_{22}^{\,Y2} & \check{I}_{23}^{\,Y1} - \check{I}_{23}^{\,Y2} \\ \check{I}_{21}^{\,Z1} - \check{I}_{21}^{\,Z2} & \check{I}_{22}^{\,Z1} - \check{I}_{22}^{\,Z2} & \check{I}_{23}^{\,Z1} - \check{I}_{23}^{\,Z2} \end{pmatrix} \tag{4}$$

The interrelation between the magnetic dipole moment of the specimen and the differential sensor signals $\vec{W}$ is given by Eq. (5).

$$S\,(\phi)\,\vec{m} = \vec{W}\,(\phi) \quad \text{with}$$
$$\vec{W}\,(\phi) = \begin{pmatrix} X1\,(\phi) - X2\,(\phi) \\ Y1\,(\phi) - Y2\,(\phi) \\ Z1\,(\phi) - Z2\,(\phi) \end{pmatrix} \tag{5}$$

Minimisation of the sum over the squared errors leads to Eq. (6) as the best estimate for the magnetic dipole moment of the considered specimen. In Eq. (6), ϕ' defines the angular interval which is used for the regression analysis of one particular sample.

In practice, linear trends and constant offsets in the differential signals were observed. The constant offsets are due to different offsets of the paired sensors and due to an adjustable offset of the amplifying electronics. Linear trends result from time-dependent external fields which can be treated linear in the considered time of approximately 2 seconds necessary for a sample to pass through the selected angular interval. To overcome these transients, six further elements were added to the matrix S. These elements are one constant term to fit constant offsets and one proportional to the rotation angle to fit linear trends for each of the three differential signals.

All calculations are done numerically. The matrix S is calculated for (the adjustable) sensor positions and the angular position of the specimen for each angular step. The steps are fixed as 500 per rotation by the rotary encoder. Matrix T (Eq. (7)) and the integral in Eq. (6) are calculated by numerical integration over the user-defined angular range from $-\phi'$ to ϕ'. The magnetic moment $\vec{m}$ is calculated subsequently by using Eq. (6).

$$\vec{m} = T^{-1} \int_{-\phi'}^{\phi'} S\vec{W} d\phi \tag{6}$$

$$T_{jk} = \int_{-\phi'}^{\phi'} S_{ij} S_{ik} d\phi \tag{7}$$

Typical signals recorded by Hotspin 2 and the fitted curves based on the result of the regression analysis are shown in Fig. 3.

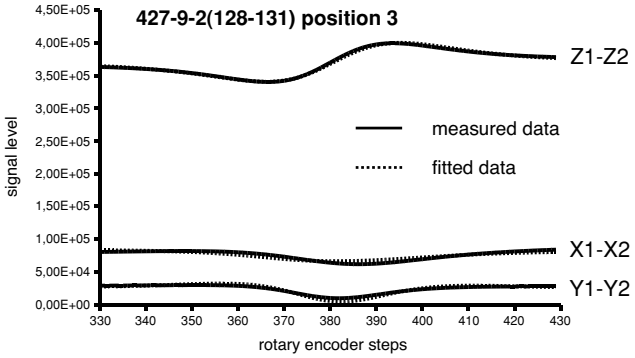

Fig. 3. Typical signals measured by Hotspin 2 for a sample fixed at encoder step 379. The signals resemble those of measured along profiles across magnetic anomalies. The constant offsets of the signals can be adjusted by the electronics and don't have an effect on the analysis of the data.

4. Results

In the following, the calibration and testing of the Hotspin 2 magnetometer and some continuous thermal demagnetisation curves of artificial and natural remanent magnetisations of oceanic basalts are described.

4.1 Calibration and testing

The Hotspin 2 instrument was calibrated using five inch-sized oceanic basalts from the Deep Sea Driling Project (DSDP) that already had an isothermal remanent magnetisation (IRM) imparted from earlier studies. A new IRM was imparted with a pulse magnetiser (by Magnetic Measurements Ltd) in a field of 1.1 T in various directions, so that one sample each had a remanence approximately along the following directions: $I = 90°$, $I = 0°$ and $D = 180°$, $I = 45°$ and $D = 0°$, $I = -45°$ and $D = 270°$, $I = -35°$ and $D = 45°$. To reduce the intensity of this IRM to a value comparable to the NRM of oceanic basalts, the samples were individually demagnetised by alternating fields of 50 mT in three orthogonal directions (degausser by 2G Enterprises) and the intensity of the resulting remanence, which is now referred to as artificial remanence, varies in the range of 3 A/m to 8 A/m. The samples were measured by Hotspin 2 at room temperature in eight different orientations, with the samples' X, Y, −X and −Y axes oriented along the instrument's x axis first for the samples' Z axis parallel to the instrument's z axis and then antiparallel. The determined intensities are plotted versus the remanence intensity as measured by a conventional spinner magnetometer (Minispin by Molspin Ltd) in four positions (Fig. 4(a)). The slope of the line through origin best fitting the data (with $R^2 = 0.98$) was used as calibration factor for Hotspin 2.

There is a dispersion in the intensity measured by Hotspin 2 for the eight different sample directions. The smallest dispersions were recognised for the samples magnetised in the Z direction and the −X direction. The mean of all directions for each sample is close to the fitted line.

The direction of remanence determined by Hotspin changed according to the chosen orientation of the sample. The dispersion of the remanence directions after correcting for the eight different orientations of the sample are shown exemplarily for specimen 427-9-2(128-131) in Fig. 4(b). The direction is more variable in declination (±10°) than in inclination (±3°), but the mean value of the eight directions (Fisher, 1953) determined is similar to the result by Minispin, where four different orientations were measured.

The hot air heating for Hotspin 2 had to be redesigned several times during the development. Maximum temperatures are still restricted to around 350°C, but that is a significant improvement compared to our initial results. A further increase in maximum temperature could be achieved by increasing the power of the heat gun and the flow of hot air by a stronger fan at the outlet for the air after the oven. A typical temperature vs. time characteristics for a measurement with Hotspin 2 from room temperature to 300°C is shown in Fig. 5. The maximum heating rate is approximately 6°C per minute and can be maintained up to 200°C. The complete run takes about three hours and typically three samples are measured simultaneously. For further tests of the temperature measurement during heating and cooling refer to Fig. 7 and Section 4.3.

4.2 Continuous thermal demagnetisation of an artificial remanence

The artificial remanence (50 mT AF demagnetisation of 1.1 T SIRM) of samples 427-9-2(128-131), 427-9-3(56-59) and 428A-4-2(76-79) was further used to test the measurements during heating and cooling. Oceanic basalt sample

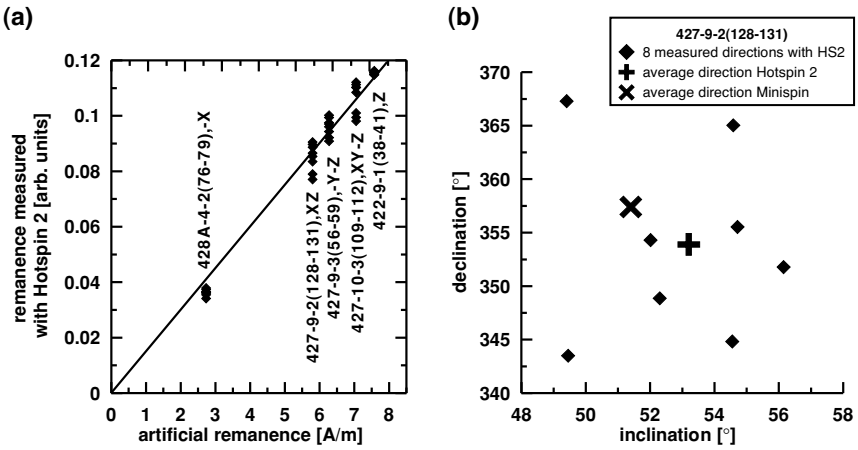

Fig. 4. Calibration of Hotspin 2. The remanence intensities determined for 5 samples in 8 orientations each with Hotspin 2 are plotted versus the intensities measured with a conventional spinner magnetometer (mean value of 4 positions), and best fitting line through origin (a). The coordinate following the DSDP sample code indicates the direction of the artificial remanence. In (b) the directions measured and corrected for 8 different orientations of sample 427-9-2 (128-131) with Hotspin 2 are plotted together with their mean direction and the direction determined with the conventional spinner magnetometer (mean value for 4 positions).

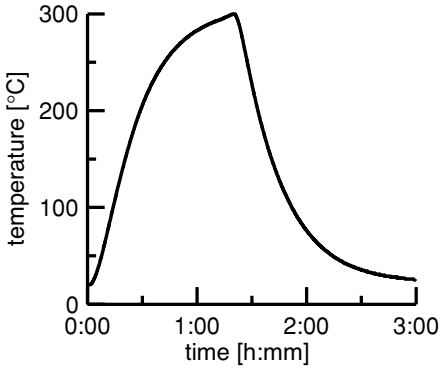

Fig. 5. Typical heating curve of Hotspin 2. Actual temperature inside the dummy specimen is plotted versus time.

427-9-2(128-131) (Minispin results: $D = 357°$, $I = 51°$, 5.8 A/m) showed a peculiar behaviour that was not observed for the other two samples. During three heating steps to maximum temperatures of 100°C, 160°C and 280°C a minimum in remanence intensity was observed at 80°C and a maximum was observed between 120°C to 150°C for each step, both during heating and cooling. During the heating step to 280°C, the declination changed by 40° and the inclination by 5° in the interval 230°C to 255°C and at room temperature the remanence intensity had dropped to half of its original value (Fig. 6(a–c)). For now it remains unclear why the direction of the remanence changed by approximately 25° during the experiment. This could be attributed to a problem of the instrument, an artefact during the acquisition of the artificial remanence, or a magnetically very stable remanence component that was unaffected by the IRM of 1.1 T (carried either by magnetically very stable goethite or hematite, however these minerals are not typical for oceanic basalts). Since the artificial remanence amounts to about only 2% (ratio determined for a sister sample) of the IRM imparted at 1.1 T, spurious magnetisation effects or comparatively strong contributions of otherwise insignificant remanence carriers like goethite and hematite might be a viable explanation.

The behaviour of interest here is the low remanence intensity between room temperature and about 150°C (Fig. 6(a)). Since it is reversible for heating and cooling, we exclude multidomain effects as described by McClelland and Sugiura (1987). Comparison with the induced magnetisation in a field of 0.679 T measured with a Variable Field Translation Balance (VFTB, Krása *et al.*, 2007) for a sister sample (Fig. 6(d)) shows that this temperature interval corresponds well to the $M_S(T)$ curve of a titanomagnetite with a Curie temperature T_C of approximately 170°C, which accounts for almost all of the sample's induced magnetisation. This suggests that the intensity minimum of the curves in Fig. 6(a) is caused by magnetisations carried by the titanomagnetite with T_C approximately 170°C, and these magnetisations, which are opposing the overall remanence direction of sample 427-9-2(128-131) might be either induced or remanent and caused by magnetic fields arising outside or inside the sample. One possible explanation for the intensity minimum therefore could be a residual magnetic field in the instrument that induces a magnetisation in the region where the sample is close to the sensors and that this field is approximately opposed to the sample's remanence. Another, less likely, possibility would be that the sample during cooling experiences magnetic fields on its circular path that lead to the acquisition of a net magnetic thermoremance opposing the total remanence. To test for these possibilities, sample 427-9-2(128-131) was again measured between room temperature and 160°C two times: first in the orientation corresponding to the previous experiments (Fig. 6(e–g)) and then with the sample oriented differently so that the vector of remanence is exactly opposite (Fig. 6(h–j)). For both experiments the intensity minimum is observed, ruling out that it is caused by magnetisations, either induced or remanent, arising from a magnetic field external to the sample. This leaves only the option that the titanomagnetite with T_C approx. 170°C acquired its magnetisation under the influence of the sample's own magnetisation, and since the

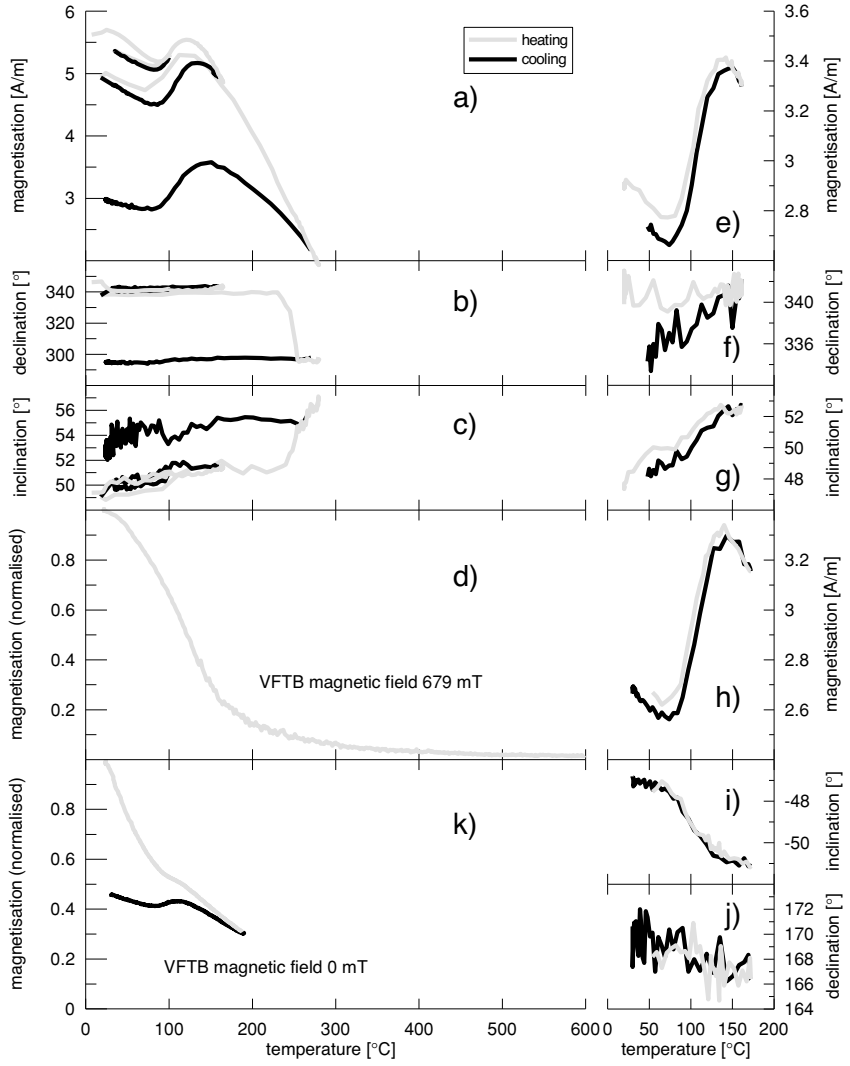

Fig. 6. Continous thermal demagnetisation of sample 427-9-2(128-131) with artificial remanence (50 mT AF after 1.1 T IRM)(a–c and e–j). Strong field thermomagnetic curve (d) and low field magnetic curve (k) measured with VFTB.

two magnetisation are opposed to each other, this behaviour can be called a partial self-reversal of magnetisation. To be sure that this apparent partial self-reversal could not be an artefact due to a problem with the Hotspin 2 instrument, a heating step to 190°C was measured for a 4 mm core in 'zero-field' in the VFTB (Fig. 6(k)). This 4 mm core was drilled from the inch-sized sample 427-9-2(128-131) after the acquisition of the artificial remanence (50 mT AF demagnetisation of 1.1 T SIRM) but before any measurements or thermal treatments with Hotspin 2. The VFTB measurement is not a true zero-field measurement, since the instruments contains an electro-magnet with pole shoes, but the field is actively compensated with a Hall probe and a coil system. Fig. 6(k) is again showing a decrease in remanence on cooling between 120°C and 80°C. This confirms, that the observed partial self-reversal of the artificial remanence is not due to an artefact of Hotspin 2.

4.3 Continuous thermal demagnetisation of oceanic basalt NRM

At present, continuous thermal demagnetisation curves between room temperature and 300°C of twenty-one oceanic basalts have been measured in batches of three samples each. Figure 7 shows the results for 22 Ma old oceanic basalts 1160B-7-1(90-92) and 1160B-9-1(119-121) from ODP Leg 187 between Australia and Antarctica (Christie *et al.*, 2001). Both samples were measured together and the directional change of the NRM is different for the two samples. Whereas 1160B-7-1(90-92) shows a change of 20° in inclination and 100° in declination during heating (Fig. 7), the NRM of 1160B-9-1(119-121) stays directionally very stable. This suggests that the measured directional changes are no artefacts, since both samples are experiencing identical conditions during continuous thermal demagnetisation in the Hotspin 2 instrument. However, we observe that the change of NRM intensity shows similarities for both samples. The intensity of the cooling curve is higher than that of the heating curve in the temperature range from about 150°C to 300°C for both samples. Usually the cooling curve would be expected to be of lower intensity due to unblocking of remanences during the thermal treatment. The remanence gain on cooling between 300°C and about 150°C is roughly parallel to the remanence direction at 300°C for both samples. Since both samples have strongly differing inclinations, again this effect could not be due to uncom-

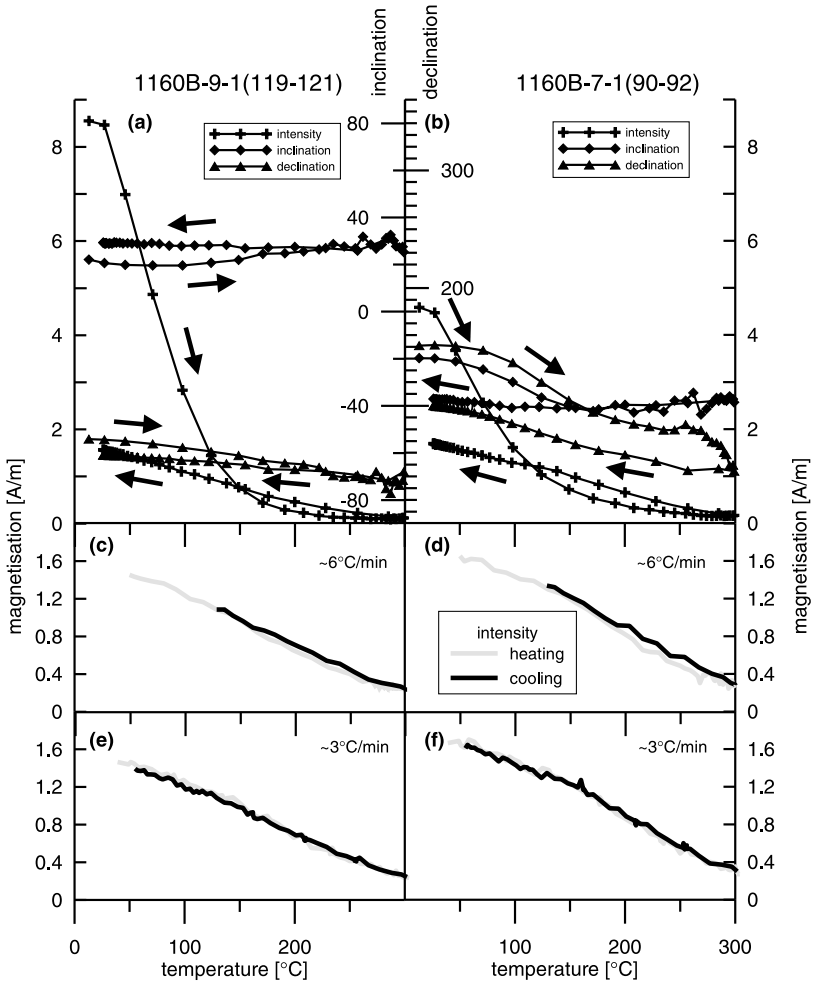

Fig. 7. Continuous thermal demagnetisation data of samples 1160B-9-1(119-121) (a), (c), (e) and 1160B-7-1(90-92) (b), (d), (f). Plots (a) and (b) are showing the first demagnetisation of the NRM including intensity and direction. The other plots show the intensity during subsequent continuous thermal demagnetisation at the full heating and cooling rate (c), (d) as well at a reduced rate of approximately 3°C per minute (e), (f).

pensated magnetic fields arising outside the sample. Another possibility could be a systematic error in the temperature measurement, with temperatures measured too low during heating and/or too high during cooling. To test for such a possibility, the previously measured samples were again heated and cooled with various heating/cooling rates. A heating/cooling run to 300°C (data not shown) was performed to better stabilise the samples (to avoid any chemical reactions within the sample during subsequent thermal treatment) and to remove potential viscous magnetisations. Heating/cooling with the maximum rate (Fig. 7(c), (d)) shows a slightly decreased magnetisation during heating that corresponds to an apparent shift in temperature between the heating and cooling curve of maximum 18°C. No such shift is observed for a heating/cooling rate of 3°C per minute (Fig. 7(e), (f)). A heating/cooling rate dependent bias of the temperature measurement, caused by e.g. thermal gradients in the samples or in the dummy sample covering the temperature sensor (or different thermal properties of samples and dummy sample), can therefore account for maximum 18°C difference error. The apparent temperature difference of 45°C between heating and cooling of the NRM (Fig. 7(a), (b)) is therefore, at least in part, likely to be caused by a magnetsation increase during the thermal treatment. Similar effects have been observed for oceanic basalts containing titanomaghemite that undergoes inversion during thermal treatment (Krása and Matzka, 2007).

5. Discussion

Magnetometers for continuous thermal demagnetisations are rare and all instruments known to us were self-built in the laboratory where they operate, most of them for a specific purpose for which they were optimised (see Section 1). The Hotspin 2 magnetometer was built for the measurement of oceanic basalt NRM, and with the aim to avoid all possible magnetic fields at the sample and sensor positions. To this end, a hot air sample heating was developed and heating runs to up to 300°C were demonstrated (note: the maximum temperature has meanwhile been increased to 400°C, measurements are routinely made to 350°C). This is not high enough to fully demagnetise most rocks since magnetite, a very common magnetic mineral, has unblocking temperatures of up to 580°C. Alternatively, an electric sample heating with a high enough ac frequency could have been used, whose magnetic field would have no effect on the fluxgate sensor signal due to low pass filtering. However, the samples to be measured would be subject to the high frequency magnetic field, too, which might influence the magnetic re-

manence, in particular close to its unblocking temperature where the coercivity of the sample is small. The hot air heating that necessitated a distance between the samples and the sensors makes Hotspin 2 comparatively less sensitive then other instruments, but the NRM of oceanic basalts is still measured comfortably. The standard inch-sized samples can easily be oriented, which is an advantage for directional studies. Although the measurement of the full vector of magnetisation is important, the directional information from Hotspin 2 is not as reliable as from other instruments, where the sample can be oriented differently during the measurement procedure. However, recent studies of oceanic basalt magnetisation show that due to processes like the inversion of titanomaghemite, the intensity of NRM can vary considerable while its direction remains constant during thermal treatment (Krása and Matzka, 2007; Matzka and Krása, in press). Hotspin 2 is ideally suited to study such processes. The Hotspin 2 was tested at room temperature and calibrated with samples of known magnetic remanence. During these tests it was recognised that the dispersion of remanence intensities measured for the same sample in different orientations could possibly depend on the remanence direction (Fig. 4(b)). This could be the effect of some still unrecognised bias. The higher dispersion of declination compared to inclination (Fig. 4(b)) could be caused by sample orientation errors in the instruments. Also, the Y component of remanence, directly influencing the declination, is likely less accurately determined than the other components since it has the smallest amplitude in the differential signal (Fig. 2(b)). Additional effects causing errors in determination of the magnetisation could be the assumption of a point sized and perfectly aligned sensor in the data analysis. The actual sensors are 20 mm long and their misalignment is $< 3.5^\circ$. It is less likely that errors due to the dipole approximation are relevant here, since they were estimated to cause angular differences of about 3° only. Continuous thermal demagnetisation of one oceanic basalt carrying an artificial remanence and two oceanic basalts carrying a NRM were shown (Figs. 6 and 7). All three cases show a remanence behaviour at high temperature that is unexpected and which would not have been detected without continuous thermal demagnetisation and the possibility to monitor both intensity and direction of the remanence simultaneously. This demonstrates that continuous thermal demagnetisation is an important method to understand oceanic basalt NRM and magnetomineralogy.

6. Conclusions

A self-built spinner magnetometer, termed Hotspin 2, was described. Its novel design as an off-axis spinner magnetometer allows to measure the full vector of magnetisation without compromising the advantages of conventional spinner magnetometers, namely the independence from sensor offsets and the possibility to stack the data. A regression analysis is used to determine the magnetic moment of the sample. The instrument was designed to have a similar sensitivity for the sample's remanence components X, Y and Z, but might be slightly less sensitive for Y than for X and Z. Advantages of the new concept are the possibility to apply a field along the Z direction and that several standard inch paleomagnetic samples can be measured simultaneously. This magnetometer was additionally equipped with a non-magnetic oven that is heated with hot air to avoid any AC magnetic fields that would arise from a heating current. This concept allows to perform continuous thermal demagnetisation experiments between room temperature and 350°C, but fails to fully demagnetise most rocks since magnetite, a very common magnetic mineral, has unblocking temperatures of up to 580°C. An advantage over similar instruments is that all samples and the temperature sensor move on identical paths in the oven, guaranteeing an identical thermal environment. The instrument was calibrated by measuring oceanic basalts with artificial remanences at room temperature. One sample with an artificial remanence showed a partial self-reversal of magnetisation below 150°C. Several tests of Hotspin 2 and a comparison measurements with another instrument were performed to demonstrate that this is no artefact of Hotspin 2 but that the sample in fact shows partial self-reversal of its artificial remanence. Further, two examples of continuous thermal demagnetisation of the natural remanent magnetisation of oceanic basalts were shown. Both samples show higher remanence intensities on cooling than on heating for temperatures above approximately 150°C.

Acknowledgments. Without Jean Pohl and Nikolai Petersen Hotspin would not have been built and Hotspin 2 would not have been designed. Karl Fabian is thanked for his interest and support in the data analysis. We thank David Krása for selecting the oceanic basalt samples and him and Maxim Alexutin for helpful discussions. Hidefumi Tanaka and the reviewers Maxim LeGoff and Hidetoshi Shibuya are thanked for their constructive and helpful comments on the original manuscript. The mechanical parts of Hotspin and Hotspin 2 were built in the departmental workshop at Ludwig-Maximilians-University Munich, where we especially want to thank Joseph Habel, Günther Hesberg, Anton Mayer and Helmut Reichl. Martin Feller, Alex Hornung and Hartwig Spitzfaden are thanked for electronics support. Bartington Instruments Ltd. kindly provided technical information on the fluxgate sensors. The oceanic basalt samples were provided by DSDP/ODP and come from sample requests by N. P., D. K. and J. M. ODP is sponsored by the U.S. National Science Foundation (NSF) and participating countries under management of Joint Oceanographic Institutions (JOI), Inc. This project was funded by the Deutsche Forschungsgemeinschaft (with grant Ma 2578/1-1).

References

Cairanne, G., F. Brunet, J. P. Pozzi *et al.*, Magnetic monitoring of hydrothermal magnetite nucleation-and-growth: Record of magnetic reversals, *American Mineralogist*, **88**, 1385–1389, 2003.

Chamalaun, F. H. and H. Porath, A Continuous Thermal Demagnetizer for Rock Magnetism, *Pageoph*, **70**, 105–109, 1968.

Christie, D. M., R. B. Pedersen, D. J. Miller *et al.*, *Proc. ODP, Init. Repts.*, **187**, 2001. Available from World Wide Web: http://www-odp.tamu.edu/publications/187_IR/187ir.htm.

Collinson, D. W., *Methods in Rock Magnetism and Palaeomagnetism*, Chapman and Hall, 1983.

Creer, K. M., Thermal demagnetization by the continous method, in *Methods in Palaeomagnetism*, edited by D. W. Collinson, K. M. Creer, S. K. Runcorn, 287 pp., Elsevier, Amsterdam, 1967.

Dräger U., M. Préevot, T. Poidras, and J. Riisager, Single-domain chemical, thermochemical and thermal remanences in a basaltic rock, *Geophys. J. Int.*, **166**, 12–32, 2006.

Fisher, R., Dispersion on a sphere, *Proceedings of the Royal Society*, **A 217**, 295–305, 1953.

Fließbach, T., *Elektrodynamik*, 3.Auflage, Spektrum Akademischer Verlag, 2000.

Gallet, Y. and M. Le Goff, High-temperature archeointensity measurements from Mesopotamia, *Earth Planet. Sci. Lett.*, **241**, 159–173, 2006.

Heiniger Chr. and F. Heller, A High Temperature Vector Magnetometer, *Geophys. J. R. astr. Soc.*, **44**, 281–287, 1976.

Irving, E., W. A. Robertson, P. M. Stott, D. H. Tarling, and M. A. Ward, Treatment of partially stable sedimentary rocks showing planar distribution of directions of magnetization, *Geophys. J.*, **66**, 1927–1934, 1961.

Kono, M., Y. Hamano, T. Nishitani, and T. Tosha, A new spinner magnetometer: principles and techniques, *Geophys. J. R. astr. Soc.*, **67**, 217–227, 1981.

Kono, M., M. Hoshi, K. Yamaguchi, and Y. Nishi, An automatic spinner magnetometer with thermal demagnetization equipment, *J. Geomag. Geoelectr.*, **43**, 429–443, 1991.

Kono, M., M. Koyanagi, and S. Kokubun, A ring-core fluxgate for spinner magnetometer, *J. Geomag. Geoelctr.*, **36**, 149–160, 1984.

Krása, D. and J. Matzka, Inversion of titanomghemite in oceanic basalt during heating, *Phys. Earth Planet. Inter.*, **160**, 169–179, 2007.

Krása, D., V. P. Shcherbakov, T. Kunzmann, and N. Petersen, Self-reversal of remanent magnetization in basalts due to partially oxidized titanomagnetites, *Geophys. J.*, **162**, 115–136, 2005.

Krása, D., K. Petersen, and N. Petersen, Variable Field Translation Balance, in *Encyclopaedia of Geomagnetism and Paleomagnetism, Series: Encyclopaedia of Earth Sciences Series*, edited by D. Gubbins and E. Herrero-Bervera, Springer, 2007.

Le Goff, M. and Y. Gallet, A new three-axis vibrating sample magnetometer for continuous high-temperature magnetization measurements: applications to paleo- and archeo-intensity determinations, *Earth Planet. Sci. Lett.*, **229**, 31–43, 2004.

Matzka, J., Besondere magnetische Eigenschaften der Ozeanbasalte im Altersbereich 10 bis 40 Ma, Ph.D. Thesis, Ludwig-Maximilians-Universität München, 2001.

Matzka, J., D. Krása, T. Kunzmann, A. Schult, and N. Petersen, Magnetic of 10-40 Ma old ocean basalts and its implications for natural remanent magnetization, *Earth Planet. Sci. Lett.*, **206**, 541–553, 2003.

Matzka, J. and D. Krása, Oceanic basalt continous thermal demagnetisation curves, *Geophys. J. Inter.*, in press.

McClelland, E. and N. Sugiura, A kinematic model of TRM acquisition in multidomain magnetite, *Phys. Earth Planet. Inter.*, **46**, 9–23, 1987.

Plenier, G., P. Camps, R. S. Coe, and M. Perrin, Absolute palaeointensity of Oligocene (28*30 Ma) lava flows from the Kerguelen Archipelago (southern Indian Ocean), *Geophys. J. Inter.*, **154**(3), 877–890, 2003.

Schmidt, P. W. and D. A. Clark, Step-wise and continuous thermal demagnetization and theories of thermoremanence, *Geophys. J. R. astr. Soc.*, **83**, 731–751, 1985.

Shcherbakov, V., E. McClelland, and V. Shcherbakova, A model of multidomain thermoremanent magnetization incorporating temperature-variable domain structure, *J. Geophys. Res.*, **98**, 6201–6216, 1993.

Shcherbakova, V. and V. Shcherbakov, Properties of partial thermoremanent magnetization in pseudosingle domain and multidomain magnetite grains, *J. Geophys. Res.*, **105**, 767–781, 2000.

Stacey, F. D., Spinner-magnetometer for thermal demagnetization experiments on rocks, *Journal of Scientific Instruments*, **36**, 355–359, 1959.

Stephenson, A., Apparatus for thermal demagnetization by the progressive method, in *Methods in Palaeomagnetism*, edited by D. W. Collinson, K. M. Creer, and S. K. Runcorn, 296 pp., Elsevier, Amsterdam, 1967.

Wack, M., Aufbau eines Hochtemperatur-Spinnermagnetometers zur magnetischen Untersuchung von Ozeanbasalten, Diploma Thesis, Ludwig-Maximilians-Universität München, 2006.

M. Wack (e-mail: wack@geophysik.uni-muenchen.de) and J. Matzka (e-mail: matzka@lmu.de)